ADVANCES IN GEOPHYSICS, VOL. 50, CHAPTER 7

A SCATTERING WAVEGUIDE IN THE HETEROGENEOUS SUBDUCTING PLATE

TAKASHI FURUMURA AND BRIAN L.N. KENNETT

ABSTRACT

The subducting plate is an efficient waveguide for high-frequency seismic waves. Such effects are often observed in Japan as anomalously large ground acceleration and distorted pattern of seismic intensity extending along the eastern seaboard of the Pacific Ocean from deep earthquakes in the Pacific plate, and Kyushu to Shikoku region from deep events in the Philippine Sea plate.

Seismograms in these high intensity zones show low-frequency ($f < 0.25$ Hz) onset for both P and S waves, followed by large, high-frequency ($f > 2$ Hz) later arrivals with a very long coda. Such observations are not explained by a traditional plate model comprising just high wave speed and low attenuation material in the slab.

A new plate model that can produce such guided high-frequency waves is characterized by multiple forward scattering of seismic waves due to small-scale heterogeneities within the plate. The preferred model requires anisotropic heterogeneity of elongated properties in the subduction slab with longer correlation distance (10 km) in the plate downdip direction and much shorter correlation distance (0.5 km) across the plate thickness. The standard deviation of P- and S-wave velocities and density from average is 3%. Such a quasi-laminated structure in the plate, which is equivalent to random distribution of anisotropic heterogeneities of elongated properties in parallel to the plate surface, can guide high-frequency signals with wavelengths shorter than the correlation distances along the plate. In contrasts, low-frequency signals with longer wavelength are not affected by the small scale heterogeneities and travel through the heterogeneous plate as a forerunner of the scattering signals.

The high wave speed property of the plate and a strong velocity gradient from the center to the outer part of the plate due to the thermal regime allows low-frequency ($f = 0.3$–0.5 Hz) seismic waves to escape into the surrounding, low wave-speed mantle by refraction of seismic waves. The net result is a frequency-dependent waveguide in the subducting plate with efficient guiding of high-frequency ($f > 2$ Hz) signals by multiple forward scattering and loss of intermediate frequency ($f = 0.3$–0.5 Hz) signals due to internal velocity gradients. Very low frequency signals ($f < 0.15$ Hz) with wavelength larger than the plate thickness are not significantly affected by the presence of the plate.

We demonstrate the presence of the frequency selective wave propagation effect from comparisons of observations from deep earthquakes that occurred recently in the Philippine Sea plate and in the Pacific plate. A good representation of the behavior of scattering waveguide is provided by 2D finite-difference calculations for seismic waves using heterogeneous slab models. The results of the simulations demonstrate that the frequency dependency of the models is quite sensitive to the thickness of the plate, and also depends on the scale lengths of heterogeneity distribution in the plate.

KEY WORDS: Seismic intensity, numerical simulation, scattering, subducting plate, waveguide.

ISSN:0065-2687
DOI: 10.1016/S0065-2687(08)00007-1

1. Introduction

Large number of earthquakes occurs in the area around Japan due to the simultaneous subduction of the Pacific plate in northern Japan and the Philippine Sea plate in western Japan (Fig. 1). Since the subducting plate acts as an efficient waveguide of

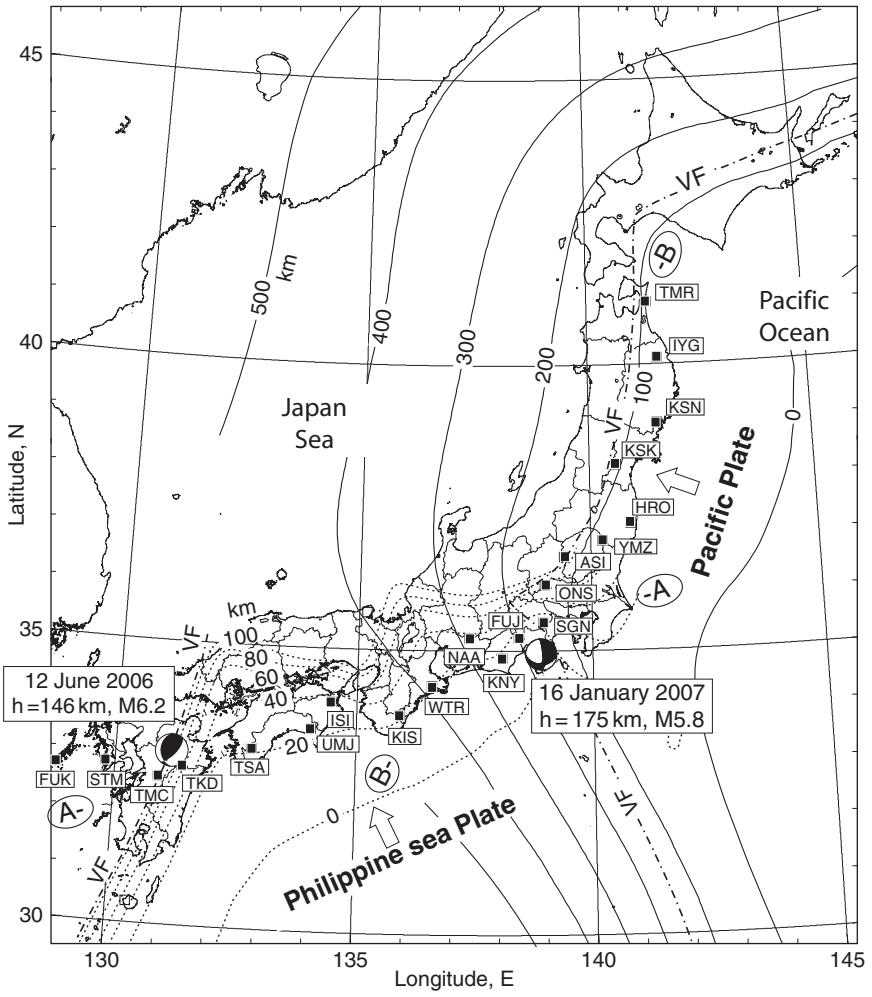

FIG. 1. The structure of the Japanese subduction zones with isodepth contours of the upper surface for the Pacific plate in northern Japan (solid curves) and for the Philippine Sea plate in western Japan (dashed curves). The associated volcanic fronts are shown with dashed lines and denoted VF. The epicenters of two events in the Philippine Sea plate on 12 June 2006 (the PHS event) and in the Pacific plate on 16 January 2007 (the PAC event) are indicated. The solid squares show the F-net broadband stations used in the analysis. A–A′ and B–B′ indicate the orientations of seismogram record sections in Fig. 3 for the PHS and PAC events, respectively.

high-frequency signals anomalously large ground motions are often produced in the fore-arc of northern Japan from intermediate to deep earthquakes occurring in the Pacific plate, and a similar effect occurs in western Japan from the earthquakes in the Philippine Sea plate. Sometimes the deep earthquakes are not felt near the epicenter, but many people are surprised by large intensities occurring in an area several hundred kilometers away from the epicenter.

Such observations of anomalously large ground motions and distorted intensity patterns for intraplate earthquakes in Japan have been recognized since modern seismic observations were started in Japan in the early 1900s (e.g. Hasegawa, 1918; Ishikawa, 1926a,b), but no satisfactory explanation for the cause of such anomalous intensity was made for over 30 years.

Utsu (1966) was the first to give an explanation. He proposed that the attenuation structure of the subduction zone in northern Japan, with a high Q and high wavespeed (high-V) dipping plate descending through a low-Q and low wavespeed (low-V) upper mantle, is the main reason for efficient propagation in the plate and so gives strong seismic signals on the fore-arc side of the subduction zone. Since then the high-V and high-Q models have been widely accepted as the expression of the subducting plate, and as a reason for the presence of high-frequency seismic waves.

Another important feature of the ground motions associated by intra-plate events are that a very long duration of high-frequency ($f > 2$ Hz) ground shaking are observed in the area of larger intensity. Such long duration and intense shaking is why people felt strong shocks from deep intra-plate earthquakes, but this type of behavior is not explained by the traditional subduction zone model comprising just a high-V and high-Q plate.

Several studies have considered the waveguide effect of high-frequency signals in the thin, low velocity zone of former oceanic crust at the top of the plate as an explanation of the time separation of low frequency arrivals from higher frequency waves, with apparent dispersion (e.g. Abers, 2000; Abers *et al*., 2003; Martin *et al*., 2003). The low velocity waveguide effect for deep ($h > 200$–500 km) Pacific plate earthquakes would be difficult to sustain, since the former oceanic crust is unlikely able to survive much beyond a depth of about 110 km without a transformation to a higher velocity eclogite. Moreover, even if the low velocity zone extended to greater depth it is still difficult to reproduce the observed large amplitudes and long duration of high frequency waves with trapped signals traveling within a thin low-Q region.

Furumura and Kennett (2005) proposed an alternative explanation of the waveguide effect for high-frequency signals in the Pacific plate by assuming strong heterogeneities in the plate. With the aid of 2D and 3D finite-difference method (FDM) simulations of seismic wave propagation they demonstrated that multiple forward scattering of high-frequency signals in the heterogeneous plate is the main cause of the guiding of high-frequency signals with very long coda. They used anisotropic heterogeneity model of von Karmann type function with a correlation length of about 10 km in downdip direction, and much shorter correlation length of about 0.5 km across the thickness, and a standard deviation of wave speed fluctuation from the average background model of 2%. This model proves to be very suitable to describe the observed characteristics of the broadband waveforms for the Pacific plate subduction zone.

The aim of this study is to review the scattering waveguide effect in the heterogeneous subduction plate through comparison between observations from dense seismic arrays of the F-net broadband and the K-NET and KiK-net strong motion instruments across Japan

for two recent earthquakes; the first occurred on 12 June 2006 in the subducting Philippine Sea plate at depth of $h = 146$ km below western Oita prefecture (M6.2), southwestern Japan (hereafter we call the PHS event) and the second on 16 January 2007 in the Pacific plate at depth of $h = 175$ km beneath the Izu Peninsula (M5.8), central Japan (hereafter the PAC event). The frequency-dependent propagation properties of the P and S waves in heterogeneous plate is demonstrated by finite-difference method (FDM) simulation of seismic waves using different classes of plate structure and internal heterogeneities in the subducting plate. Through comparisons between the observations and the computer simulations for the two events, we will examine the similarity and dissimilarity in the heterogeneous structure in the Philippine Sea plate and the Pacific plate, through such parameters as the scale length of internal heterogeneities within the plate and the thickness of heterogeneities that characterize the guiding properties of the high-frequency signals.

2. Anomalous Intensity Patterns from Two Deep Events in the Subducted Philippine Sea Plate and in the Subducted Pacific Plate

Figure 2 illustrates the distribution of peak ground acceleration (PGA) for the PHS and PAC events.

The seismic intensity scale, which was originally defined by the strength of felt shaking and the damage rate of low-rise buildings, is very sensitive to higher-frequency signals in the 0.5–2 Hz range. Thus, the anomalous pattern of intensities from intermediate and deep events is more pronounced when we map PGA rather than the peak ground velocity or the displacement. Thus, we illustrate distributions of PGA contours in Fig. 2 using the records of 3-component K-NET and KiK-net accelerograms (squares and triangles in Fig. 2).

The PGA pattern from the PHS event shows a substantial northeast-southwest elongation of isoseismic contours with the largest PGA ($>$150 cm/s/s) values at the stations in the Shikoku and Chugoku regions over 100–200 km away from the epicenter. The area of larger PGA ($>$50 cm/s/s) occurs on the fore-arc side of the volcanic front (dashed line in Figs. 1 and 2), and the PGA contours appear to be correlated with the configuration of the isodepth contours of the Philippine Sea plate (Yamazaki and Ooida, 1985). The attenuation of PGA on the back-arc side, behind the volcanic front, is very dramatic in the Kyushu and Chugoku areas. At similar epicentral distances, the PGA value in the area of raised intensity is more than 10 times larger than that behind the volcanic front.

A similar observation of an anomalous pattern of the PGA distribution is found in northern Japan associated with the PAC event as is shown in Fig. 2b. There is a significant extension of PGA contours in the northeast direction along the strike of subducting Pacific plate with largest PGA ($>$20 cm/s/s) occurring in the southern Tohoku region more than 100–200 km away from the epicenter. The extension of PGA contours along the subducting Pacific plate is more striking than for the Philippine Sea plate event, and the area where the strong motion instruments were triggered extends more than 700 km from the epicenter along the eastern seaboard of the Pacific Ocean. In contrast, only very small PGA is observed at the stations to the west of the volcanic front even at the vicinity of the epicenter.

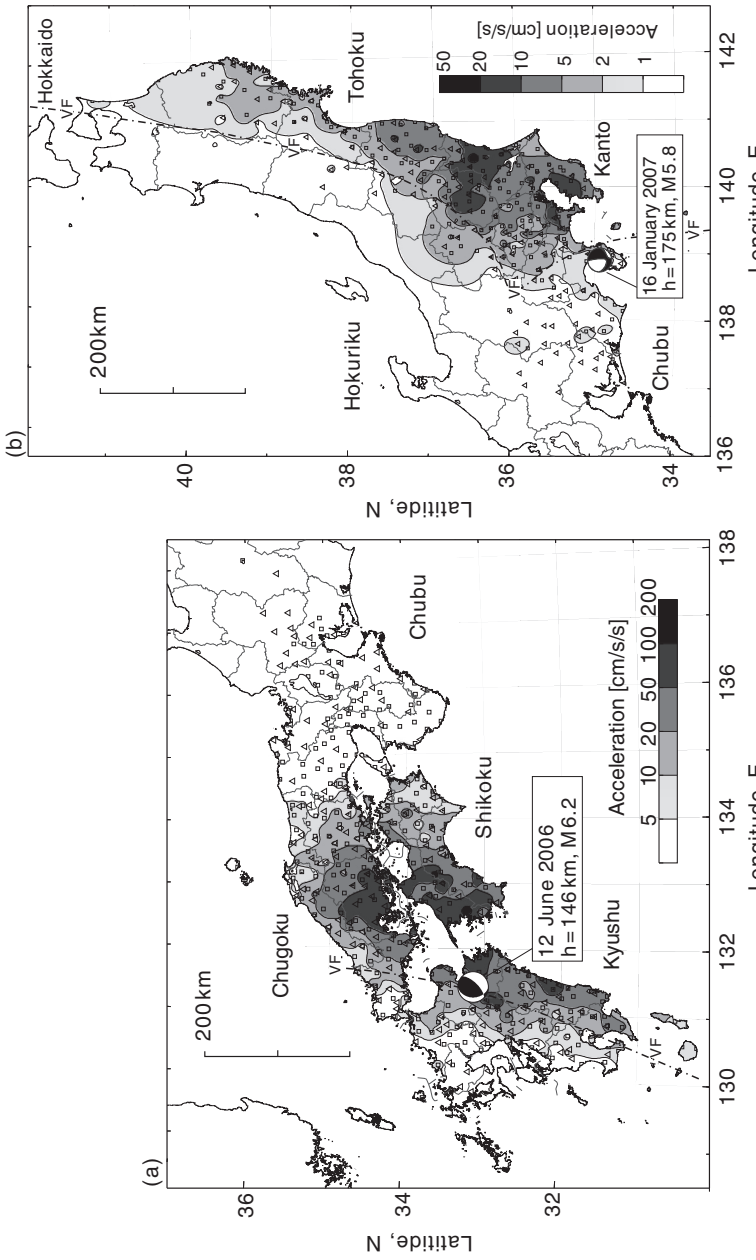

FIG. 2. The pattern of peak ground acceleration (PGA) for (a) the PHS event and (b) the PAC event. Triangles (KiK-net) and squares (K-NET) indicate the triggered stations induced by the earthquake. The location of the volcanic front (VF) is marked by dashed lines.

Figure 3 displays radial-component broadband records of ground velocity from the PHS event along a profile from Kyushu to the Chubu region (A–A′ in Fig. 1), and from the PAC event along a profile from the Chubu to Tohoku regions crossing the volcanic front (B–B′, Fig. 1). The seismic traces are multiplied by the epicentral distance to

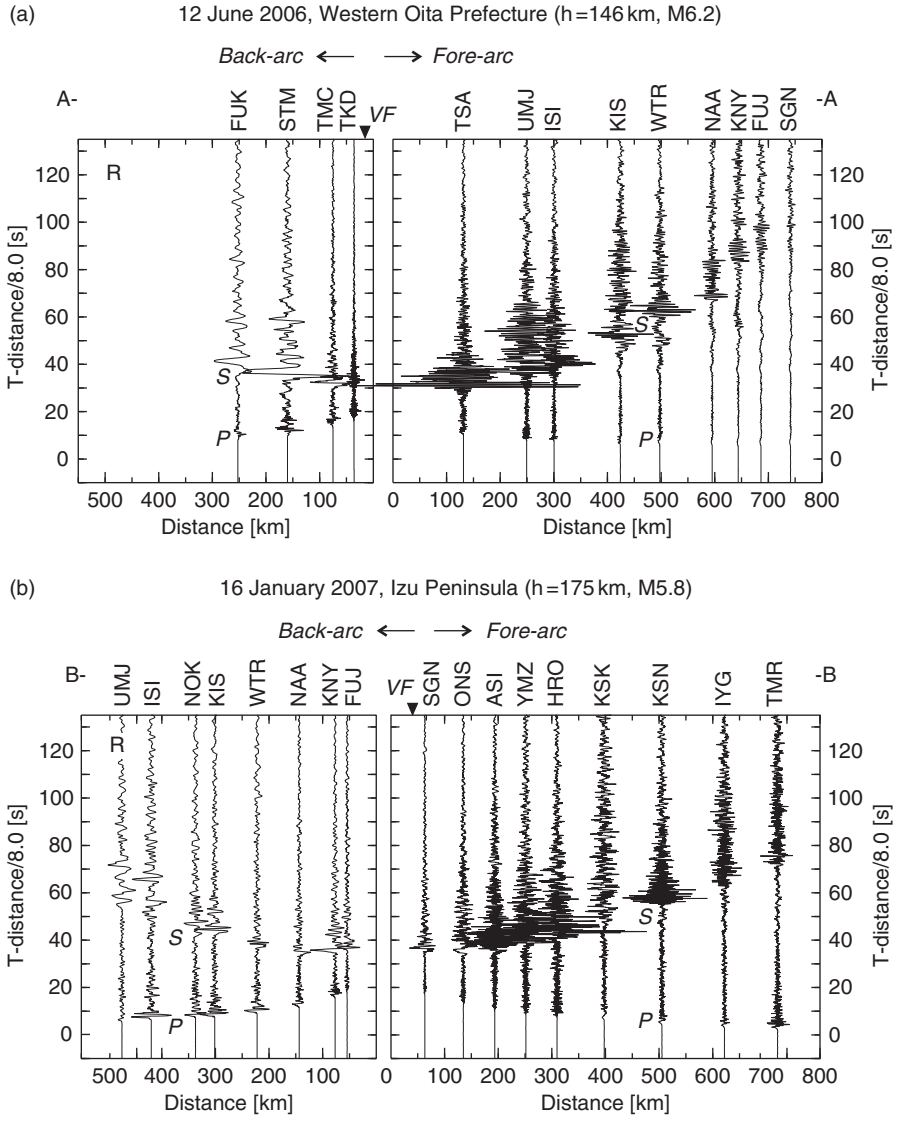

FIG. 3. Radial-component record section of ground velocity from (a) the PHS event along the profile A–A′ in Fig. 1 and (b) from the PAC event along the profile B–B′ in Fig. 1. The seismograms are recorded the labeled stations of the F-net broadband network (see Fig. 1 for locations). VF denotes the position of the volcanic front for each case.

roughly compensate the geometrical spreading of P and S body waves. The contrast in the appearance of the waveforms across the volcanic front is very striking, especially for S waves. A very large and high-frequency ($f > 1$–2 Hz) P- and S-wave signal with very long coda is observed at fore-arc stations as the wave traveling along the plate, but the attenuation of high-frequency signals is very significant in the records from back-arc stations, especially for S waves.

2.1. Separation of Low-Frequency Precursors and High-Frequency Coda

An interesting feature in the waveforms from deeper subduction zone earthquakes that cause large shocks for stations in the fore-arc region is that the seismograms show a low-frequency ($f < 0.25$ Hz) P-and S-wave onset followed by delayed high-frequency ($f > 2$ Hz) signals with a long coda (e.g., see Fig. 7 in Furumura and Kennett, 2005). This pattern seems to be a common characteristics of the waveform from major inslab earthquakes such as those occurring in the Cocos plate of Nicaragua (Abers *et al*., 2003) and the Nazca plate at the Chili-Peru subduction zone (e.g., Martin *et al*., 2003).

Figure 4 illustrates the three-component broadband waveforms at WTR for the PHS event (Fig. 4a) and at KSN from the PAC event (Fig. 4b). Both stations lie in the fore-arc for the different seduction zones. The long-period P wave precursor from these events is very clearly recognized in the radial and vertical motions with an offset of about 2 s prior to the high frequency arrivals. There is no clear precursor in tangential motion. The precursor therefore represents the direct propagation of P waves from the source to the station. The following high-frequency waves are sustained for a very long time with large amplitude, which is quite similar for all three components. This character suggests strong internal scattering of high-frequency signals due to heterogeneities in the plate. There is also large P-wave energy on the transverse component in the higher frequency part, indicating a complicated pattern of wave propagation along the heterogeneous plate.

The scattering and guiding effects for the high-frequency signals along the plate are very striking in the records from the Pacific plate event, but are not so much clear for the Philippine Sea plate. The difference may indicate stronger heterogeneities in the Pacific plate.

2.2. Frequency Selective Propagation Properties in the Subducting Plate

The contrast in the high-frequency content of the waveforms across the volcanic front of the Philippine Sea plate and of the Pacific plate are examined by taking the spectral ratio of broadband records between fore-arc and back-arc stations at comparable epicentral distances. Since the F-net stations are all placed in hard rock sites, we expect that local site amplification effects at each station can be ignored.

Figure 5a illustrates the spectral ratio of the S wave for a 24.6 s time window at the fore-arc stations NSK and TSA relative to the back-arc stations STM and SBR respectively for the PHS event. Figure 5b is a similar spectral ratio for the PAC event between the fore-arc stations ASI and ONS and the back-arc stations KNM and TGA respectively.

For the PAC event (Fig. 5a), both sets of spectral ratios show a smooth rise from about 0.15–30 as the frequency increases from 0.3 to 1 Hz, and then the rate of increase diminishes in the higher frequency band (due to the loss of higher-frequency signals at back-arc stations). The lower values in the spectral ratio (<1) in the low-frequency band below about 0.15 Hz arise from the radiation pattern of the S waves.

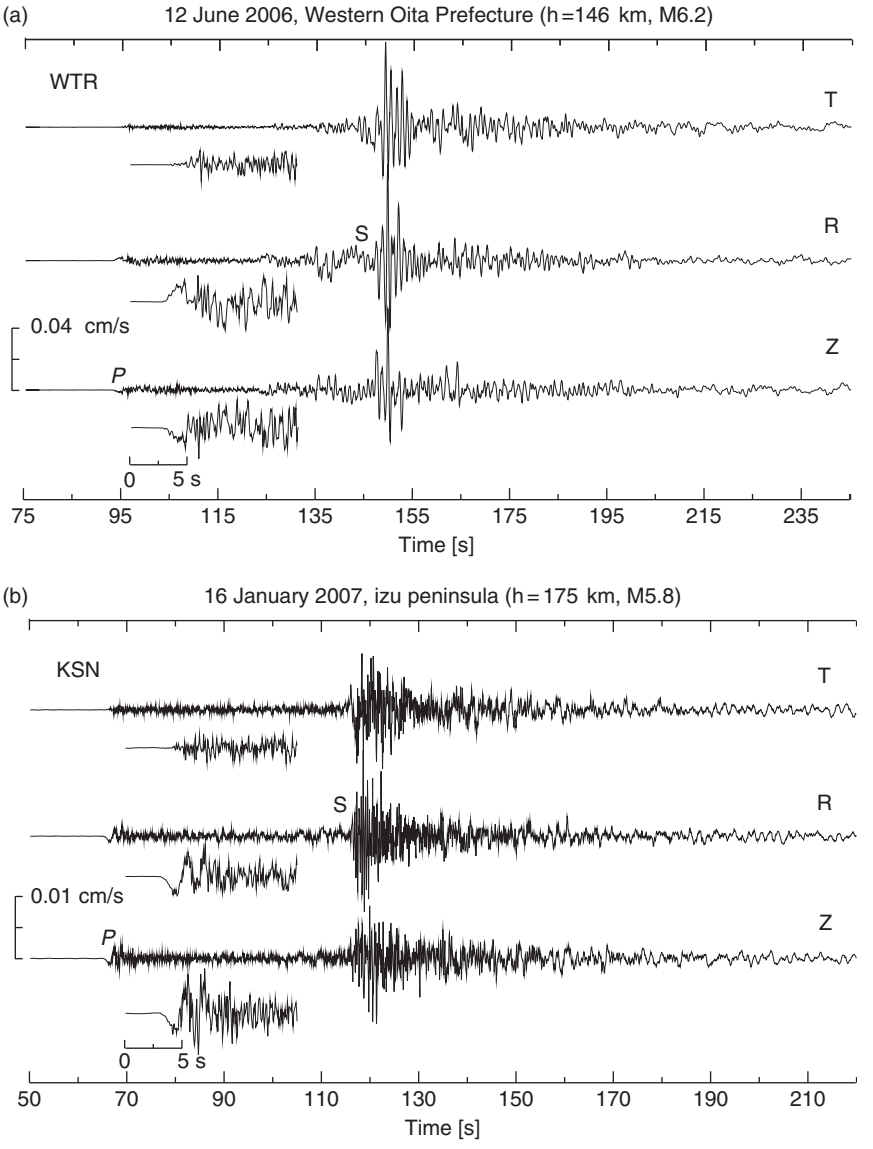

FIG. 4. Three-component broadband records of transverse (T), radial (R), and vertical (Z) motion at station (a) WTR from the PHS event and (b) at station KSN from the PAC event. Both stations are located on the fore-arc side of the subducting plate (see Fig. 1). An expanded P-wave segment for the three-component records is displayed at the left.

The guiding of high-frequency signals within the subducting Philippine Sea plate from source to fore-arc stations is clearly confirmed by Fig. 5a for frequencies above about 0.3 Hz. We have strongly frequency-dependent anelastic attenuation (Q) properties, with

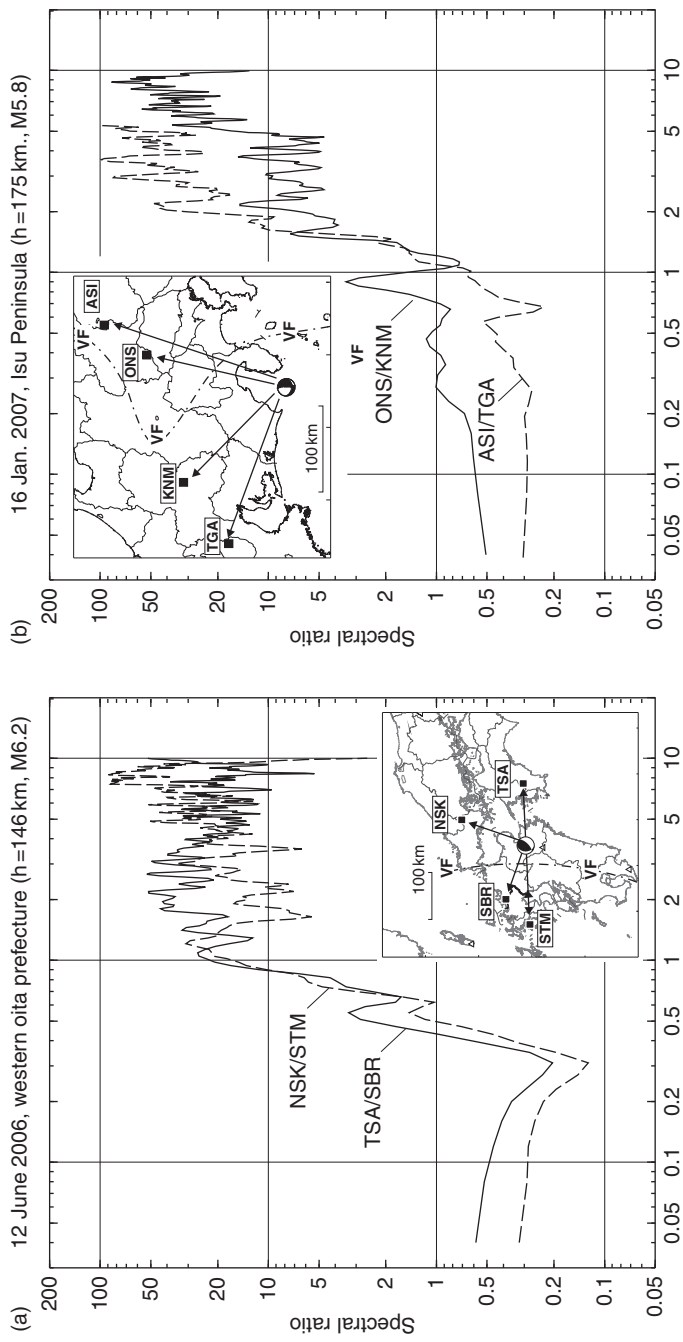

FIG. 5. Spectral ratio of broadband waveforms at fore-arc stations relative to back-arc stations for (a) the PHS event (NSK/STM and TSA/SBR) and (b) the PAC event (ONS/KNM and ASI/TGA). The locations of the F-net broadband stations are shown in the insert maps as solid squares.

an increase in Q values in the slab relative to that in the wedge mantle with increasing frequency above 0.3 Hz.

The significant drop in the spectral ratio around 0.3 Hz for the PHS event indicates that the seismic waves in this frequency band are dramatically attenuated whilst traveling up the Philippine Sea plate. The results demonstrate a complicated, frequency selective, waveguide property for the subducting plate due to strong scattering of high-frequency signals with wavelengths shorter than the heterogeneities in the plate. They also indicate escape of seismic waves from the plate in the lower frequency band. The low-frequency signals with wavelengths longer than the dominant scale of heterogeneities cannot be captured by such small-scale heterogeneities in the plate and thus easily escapes from the high-V plate to the surrounding low-V mantle.

Such a defocusing effect from the subducting plate in the low-frequency band is not so clearly observed for the PAC event (Fig. 5b). In this case there is an almost linear increase in the guiding properties of the high-frequency signals over a wide frequency range above 0.5 Hz, and no clear drop in the spectral ratio can be found in the low-frequency band below 0.5 Hz.

The difference in the frequency selective properties for the guiding of seismic signals in the Philippine Sea plate compared with the Pacific plate are likely to be related to the specific characteristics of each plate, such as plate thickness and the shape and scale lengths of heterogeneities in the plate.

3. 2D FDM Modeling of Scattering Wavefield

We illustrate that the guiding of high-frequency signals is produced by heterogeneities in the plate leading to the time separation of low- and high-frequency signals, by FDM simulation of high-frequency seismic waves in 2D heterogeneous structures.

The 2D model covers a region of 204.8 km $\times$ 204.8 km, which is discretized with a uniform grid interval of 0.1 km. The seismic wavefield is calculated explicitly by solving the equation of motions and the constitutive equations using a 16th-order staggered-grid FDM in space and 2nd-order scheme in time (Furumura and Chen, 2004).

The simulation model has P- and S-wave velocity of $V_P = 8$ km/s, $V_S = 4.6$ km/s, and density of $\rho = 2.6$ t/m^3. Frequency independent intrinsic anelastic properties for P- and S-wave with $Q_P = 2400$ and $Q_S = 1200$ are introduced in the FDM simulation using the memory variable technique of Robertsson *et al.* (1994). An absorbing boundary of Cerjan *et al.* (1985) is applied to the 20-grid points surrounding the model in order to reduce artificial reflections from model boundaries. An explosive line source with a pulse width of 10 Hz is introduced in the model, which radiates P wave isotropically.

The first simulation (Fig. 6a) employs a random media with an isotropic distribution of random fluctuation in the average P- and S-wave velocities and density following a von Karmann distribution function with a correlation distance of $a = 3$ km, Hurst number of $v = 0.5$, and a standard deviation of fluctuation from average background model of $\sigma = 4\%$. The stochastic fluctuations of elastic parameters were first produced in the wave number domain by applying a wave number filter to a sequence of random numbers, following the procedure of Frankel (1989), and then the result is transformed back into the physical domain using a Fast Fourier Transform.

Snapshots of seismic wave propagation at times $T = 8$ and 16 s from source initiation are illustrated in Fig. 6a. The scattering of seismic wavefield produced by the presence of

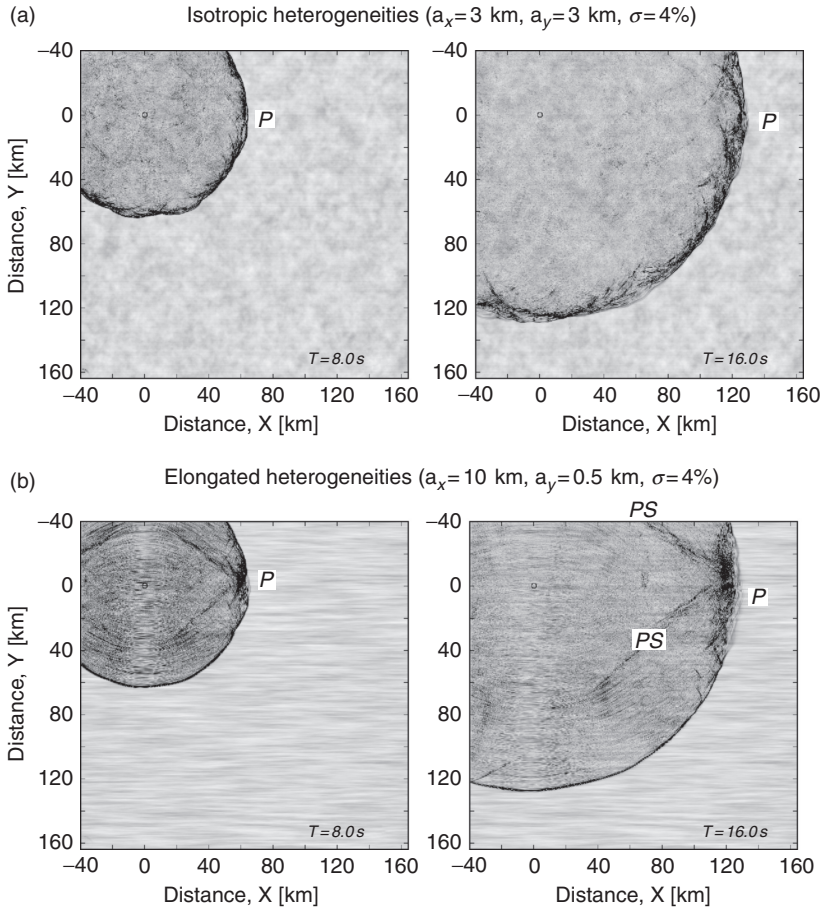

FIG. 6. Snapshots of seismic wave propagation (vector mean of two horizontal motions) at 8 and 16 s after initiation of an explosive source, derived from the 2D FDM simulation of seismic wave for models of (a) isotropic velocity fluctuation of von Karmann type function with a correlation length of $a = 3$ km and standard deviation of $\sigma = 4\%$, and (b) anisotropic, elongated heterogeneities with a correlation length of $a_x = 10$ km/$a_y = 0.5$ km, and a standard deviation of $\sigma = 4\%$. The wavefronts of P and PS converted waves are marked.

small-scale heterogeneities in the model is evident; the P wavespeed is distorted, and a strong coda is developed behind the wavefront. Such behavior resembles the patterns that are seen in the actual seismic waves observed at fore-arc stations, with an incoherent pattern of P and S phases between even close stations and an associated large coda. However, the simulation results for isotropic distribution of random heterogeneity model cannot explain the separation of the low-and high-frequency components of the initial P wave which is another important feature of the observations for intraplate earthquakes.

The second simulation assumes an elongated heterogeneity with a longer correlation distance of $a_x = 10$ km in x direction and much shorter correlation distance of

$a_y = 0.5$ km in y direction, retaining the areal scale of heterogeneity at $a_x \times a_y = 5$ km^2 with a standard deviation of fluctuations $\sigma = 4\%$.

A similar style of quasi-lamina structure in the lithosphere has been considered for the interpretation of the result of a long-range refraction experiment in the former Soviet Union using nuclear sources (e.g., Morozova *et al*., 1999) and also in modeling the oceanic crust of the subducting Nazca plate based on array observations of natural earthquakes (Buske *et al*., 2002; Patizig *et al*., 2002). These observational data and corresponding computer simulations demonstrate that high-frequency Pn and Sn signals with long tails observed in continental structure can be produced by horizontally elongated heterogeneities in the crust or uppermost mantle (e.g., Morozova *et al*., 1999; Tittgemeyer *et al*., 1999, 2000; Ryberg *et al*., 2000; Nielsen *et al*., 2003; Nielsen and Thybo, 2003).

Figure 6b shows an example of such quasi-laminated structure that produces a strong waveguide effect for high-frequency waves. The enhanced forward scattering within the quasi-lamina structure arises from successive post-critical reflections at the surfaces of the lamellae. In the snapshot of the later time frame (16 s), we find a strong concentration of P-wave energy as the wave traveling in the direction parallel to the lamellae and associated coherent P-to-S reflections in the shape of a laid "V". The two features together form a characteristic shape like a sliced mushroom. Thus, the seismic waves can travel longer distances in the direction parallel to the lamellae with only limited loss compared with the homogeneous structure and the heterogeneous model with isotropic heterogeneities as Fig. 6a.

The low-frequency precursor to the main P wavefront propagating parallel to the lamellae is clearly seen in the snapshot for the later time frame ($T = 16$ s). Multiple post-critical reflections of seismic waves in the quasi-lamina structure modify the effective wave speed for high-frequency signals, but low-frequency waves with wavelength much longer than the correlation distance ($a_y = 0.5$ km in normal to the scatterers) can easily travel through such small heterogeneities at faster propagation speed. Such generation of the low-frequency forerunner is explained as an inhomogeneous wave (Ikelle *et al*., 1993) or as a tunneling wave (Fuchs and Schulz, 1976) traveling in quasi-lamina structure.

We have also examined the development of the long-period precursors in the wavefront of the P wave using different classes of heterogeneity models with varying standard deviation of fluctuation, $\sigma = 2\%$, 4%, 6%, and 8% (Fig. 7), while retaining the same correlation length for the heterogeneities as in the previous model (Fig. 6b).

The results of the simulations demonstrate that larger velocity fluctuations with an enhanced velocity contrast across the flat interfaces of the lamellae can easily produce post-critical reflections with a smaller incident angle, and can trap high-frequency energy within the quasi-lamina structure by multiple forward scattering (Fig. 7b and c). The low frequency precursors in front of the trapped high-frequency signals are largely concentrated within the critical angle defined by the contrast for the low-to-high wave speed at the interface of lamellae. For a typical velocity contrast of $(1\sim\sigma)/(1+\sigma)$, the critical angles calculated by $i_c = \sin^{-1}((1\sim\sigma)/(1+\sigma))$ are $i_c = 73.8^o, 67.4^o, 62.5^o$, and 57.4^o for the case of velocity fluctuations of $\sigma = 2\%$, 4%, 6%, and 8% respectively (Fig. 7).

Figure 7d compares synthetic seismograms of radial and transverse components for the common source (open circle) to receiver (separation 150 km; solid square) configuration for different fluctuations of $\sigma = 2\%$, 4%, 6%, and 8%. The concentration of large seismic signals following the long-period P precursor produced by the stochastic

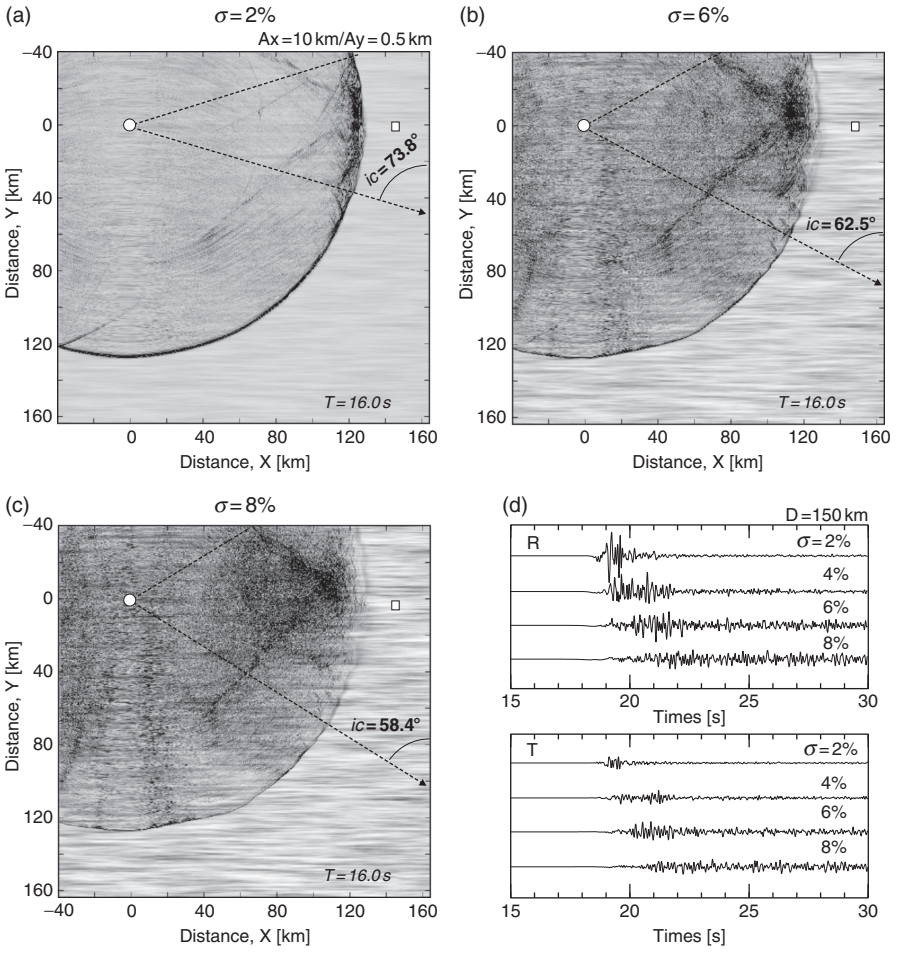

FIG. 7. Snapshots of seismic wave propagation for elongated heterogeneities ($a_x = 10$ km/$a_y = 0.5$ km) with varying standard deviation of the fluctuations, (a) $\sigma = 2\%$, (b) 6%, and (c) 8%. (d) Synthetic seismograms for radial (R) and transverse (T) motions at common stations (squares) at a distance $D = 150$ km from the source (open circle). *ic* indicates critical angle defined by the standard deviation of the velocity fluctuations across the low/high-wavespeed interface of the heterogeneities.

waveguide effect of the quasi-lamina structure is clearly demonstrated in this simulation. As the random fluctuation in elastic parameter increases, the relative amplitude of the low-frequency P wave and the duration of the coda increase very dramatically. With a large fluctuation in random heterogeneity (6–8%) the amplitude of the coda in tangential motion is almost as large as that for the P wave in radial motion. Thus, the strong concentration of P wave energy in the tangential motion from the in-slab earthquakes observed in Fig. 3 indicates the existence of strong heterogeneities in the plate.

4. 2D FDM Modeling of Slab Guided Waves

We now present 2D simulations of seismic wave propagation from in-slab earthquakes to illustrate the stochastic waveguide effect of the subducting heterogeneous plate.

The 2D model is taken along a profile cutting across Kyushu to Kanto region through the hypocenter of the PHS event which is nearly perpendicular to the subducting Philippine Sea plate (line A–A′ in Fig. 1). The physical parameters for the crust and upper mantle structure for western Japan are based on the *ak135* reference Earth model (Kennett *et al*., 1995). The shape of upper boundary of the Philippine Sea plate is based on the model of Yamazaki and Ooida (1985). The 2D numerical model covers a region of 720 km horizontally and 307 km in depth, which is discretized into 12,000 by 5120 grid points with a uniform grid interval of 0.06 km.

The simulation employs a double-couple line source with a 45° reverse fault mechanism which is placed at the depth of $h = 160$ and 5 km below the plate surface. The source radiates seismic P and S waves with a maximum frequency of 16 Hz. We conducted parallel FDM simulations using 16 nodes of the Earth Simulator which required CPU time of 65 min to simulate 240 s seismic wave propagation with 160,000 time steps in the computations.

4.1. Base Model: High-Q and High-V Subduction Zone

The first simulation employs a simple plate model with the geometry illustrated in Fig. 8, assuming a uniform velocity increase (+3%) in the descending plate relative to the *ak135* reference Earth model, while lowered (−5%) P- and S-wave velocities are assigned to the wedge mantle. We consider the thermal regime of the subducting zone with increasing temperature from the interior to the exterior of the plate. Such thermal effects in the plate can be approximated by 2% larger velocity and density at the center of the plate with a decrease to normal values toward either side of the plate, using a cosine function as shown in Fig. 8.

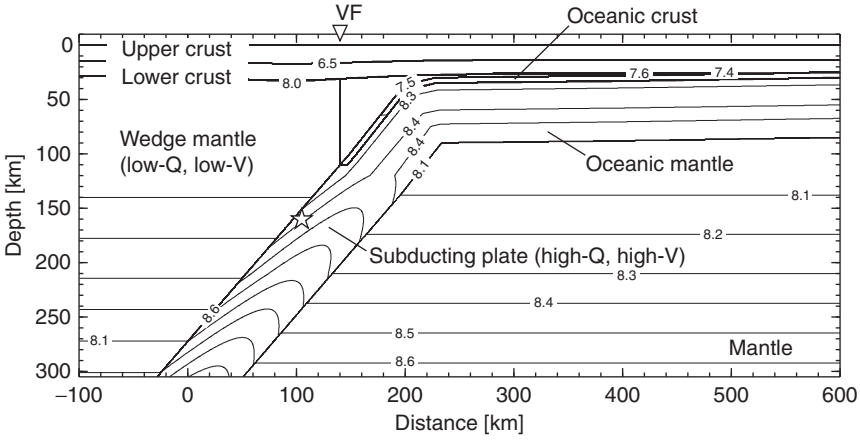

FIG. 8. 2D model of depth variation of the P wave structure used in the FDM simulation of seismic wave propagation along profile A–A′ shown in Fig. 1. Triangle and star denote the position of the volcanic front and seismic source, respectively.

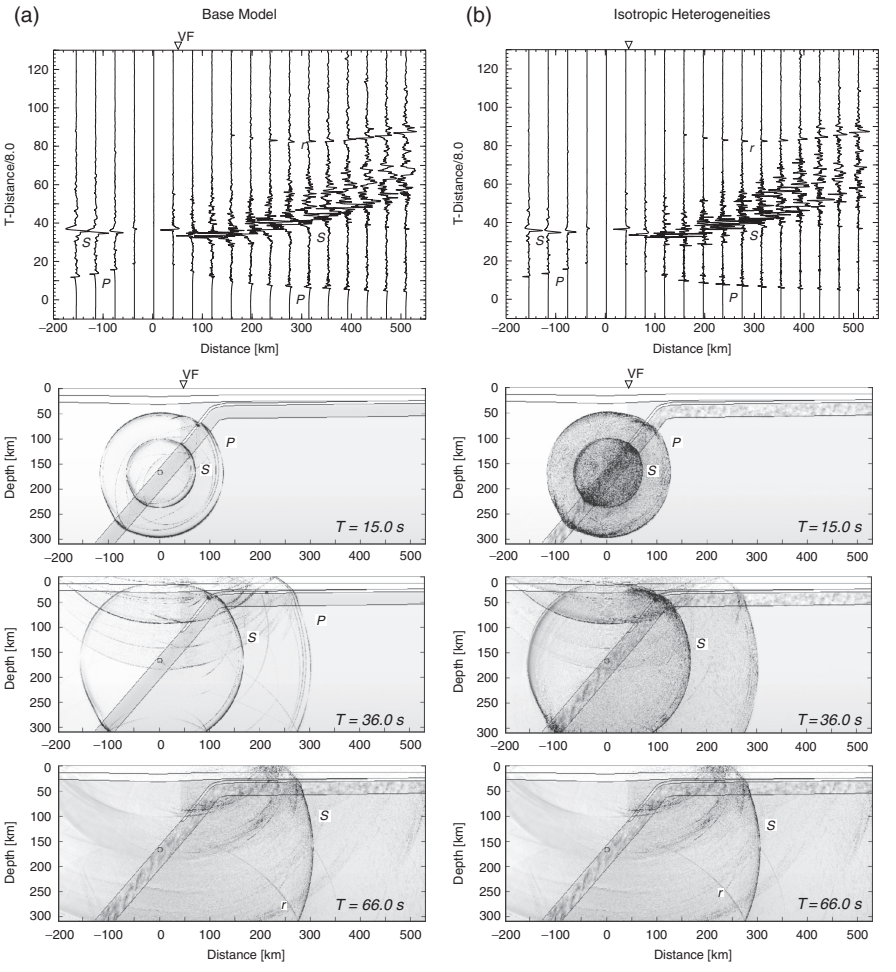

FIG. 9. Snapshots of seismic wave propagation at $T = 15$, 36, and 66 s after source initiation, and waveforms for radial motion from 2D FDM simulation. A double couple M6 event source is set in the slab at $h = 160$ km (small circle). (a) The case of base model with high-Q and high-V plate model. V_P distribution is shown in Fig. 8. (b) The case of a homogeneous, where isotropic velocity fluctuation of von Karmann type is superimposed to the base model. The correlation length is $a = 2.2$ km and standard deviation is $\sigma = 3\%$. Wavefronts of P and S waves are marked, and r indicates artificial reflections from the bottom of the model. VF denotes the position of the volcanic front.

High-Q values are assigned for P and S waves in the subducting plate ($Q_P = 2400$, $Q_S = 1200$) and somewhat smaller values for the oceanic crust ($Q_P = 400$, $Q_S = 200$). Stronger attenuation ($Q_P = 120$, $Q_S = 60$) is placed in the uppermost mantle above the plate on the back-arc side of the subduction zone, compared with that for the surrounding mantle ($Q_P = 400$, $Q_S = 200$).

The results of the FDM simulation as snapshots of seismic wavefield at $T = 15$, 36, and 66 s from the earthquake initiation are shown in Fig. 9a together with the waveforms of

radial component velocity ground motion. The synthetic seismograms are obtained by convolution with a triangular slip-velocity function assuming a rise time of $T = 0.6$ s for a M6 in-slab event.

At $T = 15$ s, the P and S waves radiated from the 160 km deep source in the plate shows a clear and nearly spherical wavefront traveling upward in the subducting plate and through the surrounding mantle. The high-Q and high-V plate brings about very large seismic signals traveling upward within the plate compared with the overlying low-Q and low-V wedge mantle.

As the P wave enters the low-V oceanic crust, trapped P waves with larger energy are built up due to the superposition of multiple reflections in the thinner low-V layer ($T = 15$ s). The P-to-SV wave conversion is striking at the top of the oceanic crust, and reduces the energy in the trapped P wave signals in the oceanic crust.

The record section of synthesized ground motions demonstrates a remarkable contrast in the shape of waveform as the volcanic front is crossed at distance of about 40 km. The waveforms at stations on the fore-arc side show large amplitude of P and S waves with dominantly higher-frequency signals. The synthetic seismograms at back-arc stations show very simple P and S pulses with a dramatic loss of high-frequency signals for waves traveling through the low-Q and low-V mantle wedges. These features are consistent with the observed broadband records (Fig. 3).

However, the guiding of high-frequency seismic signals within the plate is not strong enough in this simple model without heterogeneous plate structure. Moreover, the snapshot at $T = 15$ and 36 s show some refraction of seismic waves from plate interior to the low-V mantle outside, which gradually attenuates the seismic waves traveling in the plate.

The strong velocity gradient in the plate, caused by the thermal regime, causes significant defocusing of seismic signals from the plate center towards the surrounding mantle, resulting in very weak P- and S-wave signals at stations near the volcanic front and on the fore-arc side of the subduction zone.

The results of these computer simulations demonstrate that the traditional plate model comprised of just a high-Q and high-V plate structure cannot trap sufficient high-frequency seismic energy within the plate. Furthermore, the simulated waveforms shown in Fig. 9a seem to be too simple to explain the complex properties of the observed waveforms in the broadband records at fore-arc stations (Fig. 3), which are characterized by a very long duration of high-frequency coda.

4.2. Heterogeneous Plate Model: Isotropic Heterogeneities in the Plate

Furumura and Kennett (2005) proposed that multiple scattering of seismic wave due to heterogeneities in the plate is the main cause of large amplitude and long-duration of high-frequency P and S waves associated by in-slab zone earthquakes.

The heterogeneous plate model assumes a random media with an isotropic random fluctuation in P- and S-wave velocity and density following a von Karmann distribution function with a correlation distance of $a = 2.2$ km in all direction, Hurst number of $\nu = 0.5$ and a standard deviation of fluctuations of $\sigma = 3\%$. This random heterogeneity is imposed on the whole plate including the oceanic crust and mantle. The scale of heterogeneities are selected to produce strong seismic scattering for P waves for frequencies over $f > 2$ Hz, with average wave speed in the oceanic mantle of about $V_P = 8$ km/s and corresponding slownesses for P and S waves of 1.6 s/km and 2.7 s/km, respectively.

As is shown in Fig. 9b the high-frequency seismic wavefield is changed produced by introducing isotropic small-scale heterogeneity in the plate, especially for stations on the fore-arc side. The distortion of the P wavefront traveling though the heterogeneous plate is clearly seen in the snapshots as a result of multiple scattering of P and S waves in the heterogeneous plate. The scattering wavefield is mainly composed of the P and S multiple reflections, and P-to-SV and SV-to-P conversions are very weak in this model.

The heterogeneous plate model leads to a significant improvement in the duration of high-frequency P- and S-wave coda in the waveforms at fore-arc stations. However, the scattering of P and S waves isotropically within the plate largely dissipates seismic energy into the surrounding mantle, as is clearly seen in the snapshots at $T = 15$ and 36 s in Fig. 9b. The result is relatively weak P and S wavefronts traveling upward in the plate as compared with the homogeneous plate model of Fig. 9a. Thus, the model of internal isotropic heterogeneities in the plate produces large and long duration of P- and S-wave coda by multiple scattering, but is insufficient to keep high-frequency seismic signal within the plate.

4.3. Anisotropic Heterogeneities in the Plate

Following the study of Furumura and Kennett (2005), we improve the heterogeneous plate model by introducing a stochastic distribution of anisotropic correlation properties for the random heterogeneities in the plate. We elongate the correlation distance; $a_x = 10$ km in the downdip direction, and much shorter correlation distance of $a_z = 0.5$ km in the direction of thickness. The heterogeneity is placed in the whole plate through the oceanic crust and the oceanic mantle. Such a quasi-laminated structure produces a strong waveguide effect on high-frequency seismic signals with enhanced forward multiple P- and S-wave scattering within the plate by wide-angle reflections. This leads to a large concentration of seismic energy in the center of the plate and thus the seismic waves travel in the high-V plate with less attenuation than the previous model with isotropic correlations (Fig. 9b). The synthetic seismograms for this model with anisotropic correlations show very large P- and S-wave coda with a long duration similar to those seen in the broadband waveform of fore-arc stations (Fig. 3).

Figure 10a shows the results of FDM simulation. The scattering wavefield produced by the quasi-lamina in the plate shows a strong P-to-SV conversion following the P wave front, which is much stronger than for the earlier models with a homogeneous plate and with isotropic scatters within the plate (Fig. 9a and b). Such P-to-SV conversion associated with multiple P-wave reflections at the lamina interface removes some energy from the trapped P-wave signals within the plate, and so the trapped P-wave energy gradually leaks into the surrounding mantle by SV conversions.

For the S wave, some SV-to-P conversions associated with multiple SV-wave reflections at the interface of lamellae arise near the source region. However, such conversions to P waves disappear as the distance from the source increases, and the multiple post-critical S-wave reflections between lamellae begin to trap S-wave energy within the plate. Thus, the heterogeneous plate with a quasi-laminated plate structure acts as a perfect waveguide for S wave, but it is not so efficient for P wave. The trapped S-wave signal propagating upward in the plate is clearly seen in the snapshots in Fig. 10a. This leads to a very large and long tail for the S-wave coda in fore-arc sites.

A weak separation of a low-frequency precursor and following high-frequency later coda is found in the records at distant stations but the results of computer simulation

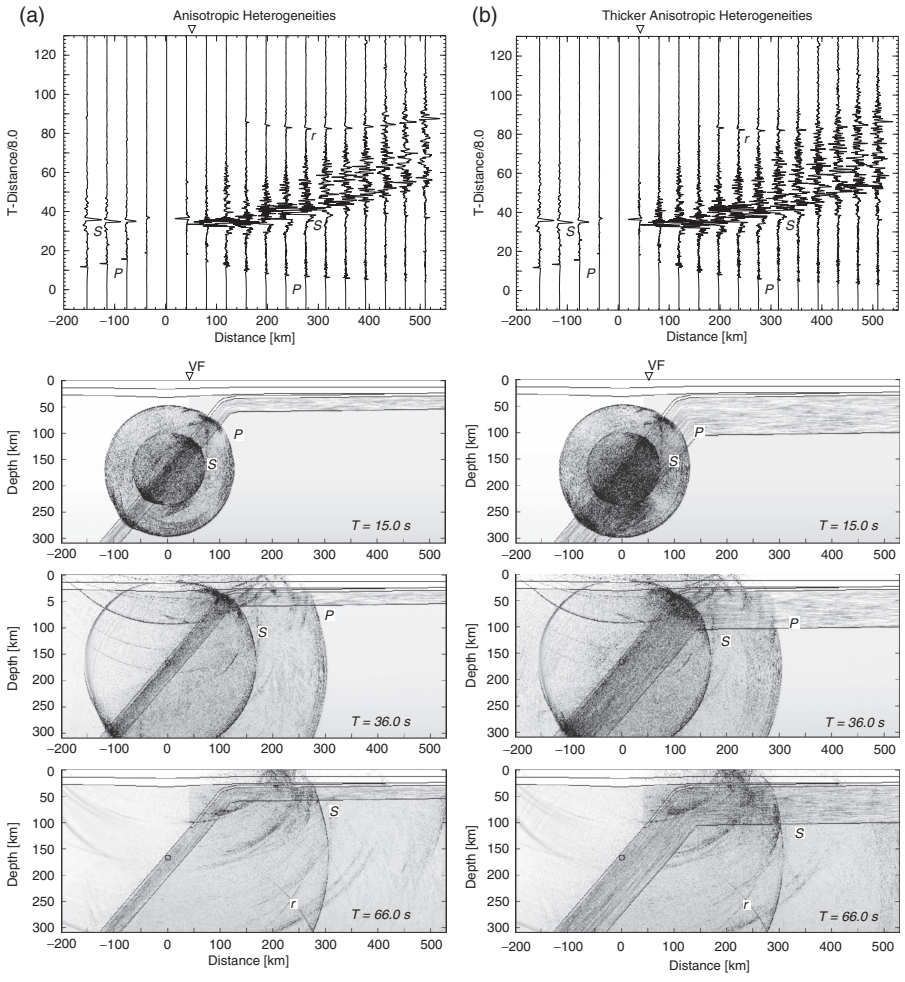

FIG. 10. Same as Fig. 9 but for a random plate model with (a) superimposed horizontally elongated anisotripic heterogeneities with a longer correlation length of $a_x = 10$ km in the downdip direction, $a_z = 0.5$ km across the thickness, and standard deviation from the average background model is $\sigma = 3\%$. (b) Thicker ($H = 85$ km) plate model with same elongated anisotropic heterogeneities.

using the present 2D subduction zone model is not as clear as the observations for Philippine Sea plate event (Fig. 3a) and as compared with the observations and corresponding simulations for the Pacific plate subduction zone event in northern Japan (Furumura and Kennett, 2005, Fig. 13). The present simulation model for the subduction zone structure in Kyushu could reproduce main feather in the broadband waveform with large and long coda in the fore-arc side stations and significant drop of high-frequency signals in the back-arc stations. However, in order for improving the

match between simulation and observed seismograms in terms of the separation of low-frequency precursor with high-frequency later code, we may need future effort to constructing proper 2D model by projection of actual 3D heterogeneous structure in the subducting zone.

4.4. Effect of Plate Thickness

The Philippine Sea plate descending below western Japan is young (30 Ma) and relatively thin (about 35–45 km), and the guiding effect of high-frequency waves within the plate tends to less effective as compared with the old (120 Ma) and thicker Pacific plate (about 80–120 km) descending below northern Japan. Moreover, the enhanced internal velocity gradient in the thinner Philippine Sea plate caused by the thermal regime, as shown in Fig. 8, tends to cause strong refraction of seismic waves towards the mantle outside.

We examine the effect of plate thickness on the guiding of high-frequency S-wave signals using a thicker ($H = 85$ km) plate model. The new plate model with a thick quasi-laminated structure leads to a strong bundle of S-wave coda trapped in the heterogeneous plate (Fig. 10b, $T = 36$ s) as compared with the thin plate model (Fig. 10a). The result is a very large S-wave with long coda traveling to fore-arc stations as we observed in the broadband seismograms for the PAC event occurring in the subducting Pacific plate (Fig. 3b). These computer simulations demonstrate clearly that the trapping properties of the high-frequency seismic waves in the heterogeneous plate are very sensitive to the shape of heterogeneities and the thickness of the waveguide.

The separation of low- and high-frequency signals in the initial P wave is slightly improved in the present simulation of thick plate model but it is still not so clear as clear as observations for the PAC event (see Figs. 3b and 4b). This may because the bending structure of the Pacific plate near the trench in Kanto region does not match to the present model for the Philippine Sea plate subduction zone in Kyushu. Note that the separation of low- to high-frequency signals in the initial P wave is very sensitive to the source and receiver configurations with the bending structure of the subducting plate. Our previous simulation of Furumura and Kennett (2005) for the model of the Pacific plate using the same elastic properties and heterogeneity distributions as the present simulation model but different configuration of the subduction zone structure demonstrated the low-frequency precursors very clearly.

As we have seen in the previous set of simulations (Figs. 6 and 7) the low-frequency P-wave precursor appears in a limited area of P wavefront. The detection of this phase may depend on the bending structure of the subducting plate and the geometry of source and receiver locations.

In order to clarify the effect of plate thickness on the guiding of high-frequency S waves within the plate, we evaluate the Fourier spectral ratio of S waves at a fore-arc station at distance $D = 100$ km, and a back arc station at the same epicentral distance ($D = -100$ km). Figure 11a compares Fourier spectral ratio of the S wave for different plate thickness of $H = 35$, 50, and 85 km.

The simulated S waves guided by the thick ($D = 85$ km) plate shows a gentle drop in the spectral ratio in lower-frequency band of about 0.2 Hz. This means that the plate is an efficient waveguide for higher-frequency signals above 0.2 Hz. The high-frequency seismic signals with wavelengths shorter than the correlation length of the heterogeneity are easily trapped in the quasi-laminated plate due to multiple post-critical S wave

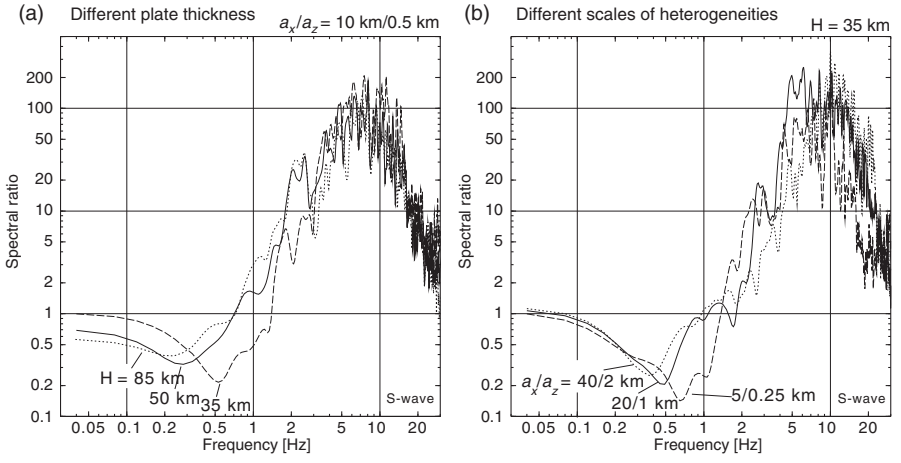

FIG. 11. Fourier spectral ratio of the synthetic seismograms of S wave at a fore-arc station ($D = 100$ km) relative to a back-arc station ($D = -100$ km) (a) for three models assuming varying plate thickness of $H = 35$, 50, and 85 km and (b) for different scales of random heterogeneities in the plate and a fixed plate thickness of $H = 35$ km.

reflections within the plate, but very low-frequency signals with longer wavelength are not sensitive to the internal structure of the plate.

A trough in the spectral ratio at frequencies between 0.15 and 0.5 Hz for the different plate thickness models arises from the anti-waveguide effect of the High-V plate with a large internal velocity gradient induced by the thermal regime. The simulation results demonstrate that the peak frequency for the anti-waveguide effect of the plate moves gradually to lower frequencies from 0.5 to 0.2 Hz as the thickness of the plate increases from $H = 35$ to 85 km.

When comparing the simulation results with observation, the spectral ratio of S waves for the PHS event (Fig. 4a) roughly corresponds to the characteristics for the plate thickness of $H = 50$ km. The case of the PAC event (Fig. 4b) roughly correlates with the simulation result for thick ($H = 85$ km) plate model, inconsistent to the thick Pacific plate descending below Kanto region.

4.5. Effect of Heterogeneity Scale in the Plate

In the simulations with varying plate thickness we have so far fixed the scale of random heterogeneity in the plate; correlation distance of $a_x = 10$ km in the plate downdip direction and $a_z = 0.5$ km in the direction of thickness. However, the frequency-selective propagation characteristics in the subducting plate are also influenced by the distribution properties of the heterogeneities within the plate.

We have conducted a set of additional simulation experiments to examine how the correlation scales of the randomness in the plate modify the propagation of high-frequency waves by multiple internal scattering within the plate. We consider three stochastic random media with varying correlation distances of nonisotropic heterogeneities with an elongated correlation distances in the plate downdip direction (a_x) and in the

plate thickness direction (a_z); (a) $a_x/a_z = 5$ km/0.25 km, (b) $a_x/a_z = 20$ km/1 km, and (c) $a_x/a_z = 40$ km/2 km. All models have the same aspect ratio of 20 and a standard deviation from the background of $\sigma = 3\%$.

The Fourier spectral radio of S waveforms in the fore-arc relative to that for the back-arc station at same epicentral distance ($D = \pm 100$ km) are compared in Fig. 11b. Simulation results demonstrate that shift of the minimum frequency of S waves, that can be trapped within the plate, varies with changes in heterogeneity scale.

As we can see from Fig. 11b, there is strong tradeoff between the plate thickness and the heterogeneity scale on the frequency-dependent waveguide properties of the subducting plate wave. The present configurations provide a reasonable representation of the observed behavior, but it is difficult to pin down the heterogeneity distribution closely from limited observational waveform data.

5. Discussion and Conclusion

Since the extensive studies of Utsu (1966, 1967, 1969) and Utsu and Okada (1968), it has been recognized that the anomalous patterns of seismic intensity from in-slab earthquakes are caused by the guiding of high-frequency waves though the high-Q and high-V plate. However, a simple plate model comprising just a high-Q and high-V plate does not explain the frequency-dependent propagation characteristics of observed seismic waves and the long coda following the P- and S-waves. In particular, the high-V property of the plate tends to shed waves from the plate because strong internal velocity gradient refract seismic energy to the mantle outside. Such anti-waveguide effects are more significant for the thin Philippine Sea plate than for the thick Pacific plate.

To solve the difficulties of past models, Furumura and Kennett (2005) proposed a new heterogeneous, quasi-laminated plate model, which is described by a non-isotropic heterogeneity in the plate structure. This heterogeneity generates trapped high-frequency ($f > 2$ Hz) waves that propagate along the plate due to multiple forward scattering within the plate. Low-frequency ($f < 0.25$ Hz) waves, with longer wave length can easily tunnel through the lamella features without affecting small scale heterogeneities or as the inhomogeneous waves with the incidence angle larger than the critical angle or as the tunneling waves (Fuchs and Schulz, 1976). The result is a separation of a low-frequency precursor and following high-frequency later signals with a long coda.

Such a non-isotropic heterogeneity structure in the subducting plate appears to be an intrinsic property of the oceanic lithosphere. Such heterogeneity may most likely be produced at the mid-ocean ridge with injection and underplating as the lithosphere is formed, and as the oceanic plate travel from the ridge to the subduction zone.

The trapping effect of the high-frequency signals for the thin ($H = 35$ km) Philippine Sea plate is somewhat weaker than for the thick ($H = 85$ km) Pacific plate, and this may be the reason for the less clear pattern of stretched intensity contours along the subducting Philippine Sea plate in western Japan compared with the clear pattern of anomalous intensity along the Pacific coast from the Pacific plate events in northern Japan.

Numerical 2D simulations of seismic P and S waves for the heterogeneous quasi-lamina plate structure demonstrate clearly how such frequency-dependent properties can arise, and how they bring about strong dependence on the velocity gradient in the plate,

the thickness of the plate heterogeneities, and the character of the heterogeneity distribution in the plate.

The present simulations are for a 2D model assuming that the source and structure are invariant in the out-of-plane direction, and thus they can account only for the scattering effects in the in-plane motion. The exclusion of out-of-plane scattering that will occur in the actual full 3D scattering situation may underestimate the amplitude and duration of P- and S-wave coda. We can reproduce the main features of the observed seismic wavefield in the present 2D modeling using suitable stochastic random heterogeneities in the plate, but before reaching firm conclusions we may need to improve the understanding of the nature of actual 3D heterogeneous wavefield. The further study should include analysis of dense seismic array data, and corresponding high-resolution 3D simulations with the aid of high-performance computing technologies.

ACKNOWLEDGMENTS

The computations were conducted as a joint science research project "Seismic wave propagation and strong ground motion in heterogeneous 3D structure" between the Earthquake Research Institute, University of Tokyo and the Earth Simulator Center. A part of CPU time was supported by the JST-CREST Project on "Multi-scale and multi-physics simulation". We acknowledge the National Research Institute for Earth Science and Disaster Prevention (NIED) for the use of K-NET and KiK-net strong motion records and F-net broadband waveform data. We thank for careful review and constructive comments from Profs. M. Ohtake, H. Sato, and S.G. Shapiro were very helpful for revision of the manuscript.

REFERENCES

Abers, G.A. (2000). Hydrated subducted crust at 100–250 km depth. *Earth Planet. Sci. Lett.* **176,** 323–330.

Abers, G.A., Plank, T., Hacker, B.R. (2003). The wet Nicaraguan slab. *Geophys. Res. Lett.* **30,** doi: 10.1029/2002GL015649.

Buske, S., Luth, S., Meyer, H., Patizig, R., Reichert, C., Shapiro, S., Wigger, P., Yoon, M. (2002). Broad depth range seismic imaging of the subducted Nazca Slab, North Chile. *Tectonophysics* **350,** 273–282.

Cerjan, C., Kosloff, D., Kosloff, R., Reshef, M. (1985). A nonreflecting boundary condition for discrete acoustic and elastic wave equations. *Geophysics* **50,** 705–708.

Frankel, A. (1989). A review of numerical experiments on seismic wave scattering. *Pure Appl. Geophys.* **131,** 639–885.

Fuchs, K., Schulz, K. (1976). Tunneling of low-frequency waves through the subcrustal lithosphere. *J. Geophys.* **42,** 175–190.

Furumura, T., Chen, L. (2004). Large scale parallel simulation and visualization of 3-D seismic wavefield using the Earth Simulator. *Comput. Model. Eng. Sci.* **6,** 153–168.

Furumura, T., Kennett, B.L.N. (2005). Subduction zone guided waves and the heterogeneity structure of the subducted plate: Intensity anomaly in northern Japan. *Geophys. Res.* **110,** doi: 10.1029/2004JB003486.

Hasegawa, K. (1918). An earthquake under the Sea of Japan. *J. Meteorol. Soc. Jap.* **37,** 203–207 (in Japanese).

Ikelle, L., Yung, S.K., Daube, F. (1993). 2D random media with ellipsoidal autocorrelation functions. *Geophysics* **58,** 1359–1372.

Ishikawa, T. (1926a). On the abnormal distribution of felt areas of an earthquake. *J. Meteorol. Soc. Jpn. Ser. 2* **4,** 137–146 (in Japanese).

Ishikawa, T. (1926b). On seismograms of earthquakes exhibiting abnormal distribution of seismic intensities. *Quart. J. Seismol.* **2,** 7–15 (in Japanese).

Kennett, B.L.N., Engdahl, E.R., Buland, R. (1995). Constraints on the velocity structure in the Earth from travel times. *Geophys. J. Int.* **122,** 108–124.

Martin, S., Rietbrock, A., Haberland, C., Asch, G. (2003). Guided waves propagating in subduced oceanic crust. *J. Geophys. Res.* **108,** doi: 10.1029/2003JB002450.

Morozova, E.A., Morozov, I.B., Smithson, S.B., Solodilov, L.N. (1999). Heterogeneity of the uppermost mantle beneath Russian Eurasia from the ultra-long range profile QUARTZ. *Geophys. Res. Lett.* **104,** 20329–20348.

Nielsen, L., Thybo, H. (2003). The origin of teleseismic Pn waves: Multiple scattering of upper mantle whispering gallery phases. *J. Geophys. Res.* **108,** 2460, doi: 10.1029/2003JB002487.

Nielsen, L., Thybo, H., Levander, A., Solodilov, N. (2003). Origin of upper-mantle seismic scattering—evidence from Russian peaceful nuclear explosion data. *Geophys. J. Int.* **154,** 196–204.

Patizig, R., Shapiro, S., Asch, G., Giese, P., Wigger, P. (2002). Seismogenic plane of the northern Andean Subduction Zone from aftershocks of the Autofagasta (Chili) 1955 earthquake. *Geophys. Res. Lett.* **29,** doi: 10.1029/2001GL013244.

Robertsson, J.O.A., Blanch, J.O., Symes, W.W. (1994). Viscoelastic finite-difference modeling. *Geophysics* **59,** 1444–1456.

Ryberg, T., Tittgemeyer, M., Wenzel, F. (2000). Finite-difference modelling of P-wave scattering in the upper mantle. *Geophys. J. Int.* **141,** 787–800.

Tittgemeyer, M., Wenzel, F., Ryberg, T., Fuchs, K. (1999). Scales of heterogeneities in the continental crust and upper mantle. *Pure Appl. Geophys.* **156,** 29–52.

Tittgemeyer, M., Wenzel, F., Fuchs, K. (2000). On the nature of Pn. *J. Geophys. Res.* **105,** 16173–16180.

Utsu, T. (1966). Regional difference in absorption of seismic waves in the upper mantle as inferred from abnormal distribution of seismic intensities. *J. Fac. Sci. Hokkaido Univ. Ser. VII* **2,** 359–374.

Utsu, T. (1967). Anomalies in seismic wave velocity and attenuation associated with a deep earthquake zone (I). *J. Fac. Sci. Hokkaido Univ. Ser. VII* **3,** 1–25.

Utsu, T. (1969). Anomalous seismic intensity distributions in western Japan. *Geophys. Bull. Hokkaido Univ.* **21,** 45–51 (in Japanese).

Utsu, T., Okada, H. (1968). Anomalies in seismic wave velocity and attenuation associated with a deep earthquake zone (II). *J. Fac. Sci. Hokkaido Univ. Ser. VII* **3,** 65–84.

Yamazaki, F., Ooida, T. (1985). Configuration of subducted Philippine Sea plate beneath the Chubu district, central Japan. *Zishin* **38,** 193–201 (in Japanese).